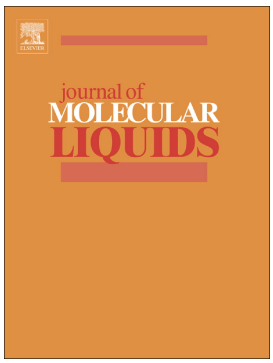

Synthesis of new low-viscous sulfonic acid-functionalized ionic liquid and its application as a Brönsted liquid acid catalyst for the one-pot mechanosynthesis of 4H-pyrans through the ball milling process

Nader Ghaffari Khaligh, Taraneh Mihankhah, Mohd Rafie Johan

PII: S0167-7322(18)34719-6
DOI: https://doi.org/10.1016/j.molliq.2019.01.024
Reference: MOLLIQ 10255

To appear in: *Journal of Molecular Liquids*

Received date: 13 September 2018
Revised date: 31 December 2018
Accepted date: 4 January 2019

Please cite this article as: Nader Ghaffari Khaligh, Taraneh Mihankhah, Mohd Rafie Johan , Synthesis of new low-viscous sulfonic acid-functionalized ionic liquid and its application as a Brönsted liquid acid catalyst for the one-pot mechanosynthesis of 4H-pyrans through the ball milling process. Molliq (2018), https://doi.org/10.1016/j.molliq.2019.01.024

Synthesis of new low-viscous sulfonic acid-functionalized ionic liquid and its application as a Brönsted liquid acid catalyst for the one-pot mechanosynthesis of 4*H*-pyrans through the ball milling process

Nader Ghaffari Khaligh[a,*], Taraneh Mihankhah[b], Mohd Rafie Johan[a]

[a] *Nanotechnology and Catalysis Research Center,3rd Floor, Block A, Institute of Postgraduate Studies, University of Malaya,50603 Kuala Lumpur, Malaysia*
[b] *Environmental Research Laboratory, Department of Water and Environmental Engineering, School of Civil Engineering, Iran University of Science and Technology, 16765-163, Tehran, Iran*

ARTICLE INFO

Article history:
Received
Received in revised form
Accepted
Available online

Keywords:
Sulfonic acid-functionalized ionic liquid
Ball mill
Pyrano[4,3-*b*]pyran
Dihydropyrano[3,2-*c*]chromene
Tetrahydrobenzo[*b*]pyran
Metal and solvent-free conditions

ABSTRACT

In the present study, a new low-viscous sulfonic acid-functionalized ionic liquid (SAIL) *viz.* 4,4'-trimethylene-*N*,*N*'-sulfonic acid-dipiperidinium chloride was synthesized and characterized by FTIR, 1D and 2D NMR, and Mass spectra. Then, some properties of new SAIL were determined including pH, viscosity, density, and solubility in some common solvents. The catalytic activity of new SAIL was demonstrated for the one-pot mechanosynthesis of pyrano[4,3-*b*]pyrans, dihydropyrano[3,2-*c*]chromene and tetrahydrobenzo[*b*]pyrans using planetary ball mill under solvent-free conditions. This current mechanosynthesis methodology for the synthesis of 4*H*-pyran-annulated heterocyclic scaffolds displays a combination of the synthetic virtues of conventional multi-component reaction with ecological benefits and convenience of a simple mechanocatalytic procedure. New SAIL was easily recycled and reused several times with no significant loss of activity.

1. Introduction

Ionic liquids (ILs) are interesting chemicals in chemistry research due to their diverse properties such as low volatility, thermal and chemical stability which makes them appropriate catalyst/solvent for the working in both high-temperature and high-vacuum conditions. ILs can often be separated from the desired organic products using a simple workup which lead to avoid high volumes of toxic and volatile organic solvents. Their applications are continuing to grow exponentially in all fields of pure and applied chemistry due to their chemical tenability, which allows different properties of ILs can tailor by an appropriate selection of anion/cation components and functional groups. ILs are promising media in liquid-liquid extraction processes and electrochemical devices such as batteries, fuel cells, sensors, and electrochromic windows. Owing to the high spectral transparency and good solvating properties of ILs, they can be suitable solvents for spectroscopic measurements. ILs have also been applied in the lubricants, plasticizers, organic synthesis, mass spectroscopy, manufacture nano-materials, and gas absorption [1-5]. Therefore, the design and synthesis of new ionic liquids and investigation of their applications are attractive and growing [6-14].

Mechanochemistry has been developed as a clean approach to the chemical transformations which minimize using of toxic and volatile organic solvents and reduce environmental pollution [15]. The milling process as a solid-state process plays a significant role in a solvent-free organic synthesis which can lead to improvements including the reduced amount of catalyst loading, shorter reaction time, and higher yield; furthermore, it fits well with the principles of green chemistry [16]. Planetary ball mills have been utilized in laboratories for the

* Corresponding author Tel.: +60-03-7967-6267; Fax: +60-03-7967-6956; E-mail: ngkhaligh@gmail.com and also ngkhaligh@um.edu.my

synthesis of catalysts [17], metal complexes [18], Schiff bases [19,20], C–C bond formation reactions, the protection of the functional groups, the preparation of the fullerenes, and redox processes [21].

4*H*-pyran-annulated heterocyclic scaffolds have been received the great attention of chemists both from the academic organizations and pharmaceutical industries due to a wide array of biological activities, particularly against cancer [22]. Based on the *in vitro*, *in vivo*, and *in silico* experiments, 4*H*-pyran scaffolds could be heterocycle candidates with potentially exploitable structures and diverse biological properties for the development of new cytotoxic and anticancer agents [23]. Fused 4H-pyran derivatives such as pyrano[4,3-*b*]pyrans constitute the core of valuable compounds exhibiting a broad spectrum medicinal and pharmacological properties including antiviral and antileishmanial [24], anticonvulsant and antimicrobial [25], anti-HIV, antituberculosis, antifungal agents [26,27], antitumor and antioxidant [28]. Therefore, a wide variety of catalysts were developed for the synthesis of these versatile and valuable compounds; for example: [bmim][BF_4] [24], NH_4OAc [28], KF/Al_2O_3 [29], triethyl benzyl ammonium chloride [30], piperidine [31], magnesium oxide [32], DBU [33], $H_6P_2W_{18}O_{62}.18H_2O$ [34], nano-eggshell/$Cu(OH)_2$ [35], thiourea dioxide [36], 4-(succinimido)-1-butane sulfonic acid [37], nano CaO [38], 1,1'-Butylenebis(3-methyl-3*H*-imidazol-1-ium) dihydrogen sulfate {[BBMIm]($HSO_4)_2$} [39], electro-catalysis [40] and alum [41].

However, the aforementioned catalysts and their methodologies have some of drawbacks such as long reaction times, moderate yields, expensive reagents, use of toxic and volatile organic solvents, and generate a waste containing metals and transition metal. Also, Lewis acids are not desirable for the synthesis of pharmaceutical products owing to their toxicity [42].

In pursuit of our studies on the preparation of new SAILs and their applications as solvent or/and catalyst in the various organic transformations [43-46], herein, a new low-viscous sulfonic acid-functionalized ionic liquid (SAIL) was designed and synthesized. The structure of new SAIL was characterized by FTIR, ^{1}H NMR, ^{13}C NMR, ^{1}H,^{1}H-COSY, ^{1}H,^{13}C-HMBC, and Mass spectra as well as its physical properties were determined. The Low viscosity, good conductivity, and the presence of two cation centers linked by alkyl spacer along with two exchangeable anions are the most interesting features of the new SAIL, and related works are underway in our laboratory. The catalytic efficiency of new SAIL was demonstrated for the synthesis of 4*H*-pyran-annulated heterocyclic scaffolds using ball milling process. We are trying our best to investigate more reactions by using this new SAIL as a solvent or/and catalyst.

2. Results and Discussion

2.1. Synthesis of 4,4'-trimethylene-N,N'-sulfonic acid-dipiperidinium chloride [TMDPS] and the characterization of its structure

4,4'-trimethylene-*N*,*N*'-sulfonic acid-dipiperidinium chloride [TMDPS] was prepared through the treatment of 4,4'-trimethylene-dipiperidine [TMDP] with two equivalents of neat chlorosulfonic acid in CH_2Cl_2 and the mixture was stirred at 50 °C overnight. The resulting ionic liquid was isolated as a low-viscous pale yellow liquid which its structure was characterized by FTIR, ^{1}H and ^{13}C NMR, ^{1}H,^{1}H-COSY, ^{1}H,^{13}C-HMBC, and Mass spectra.

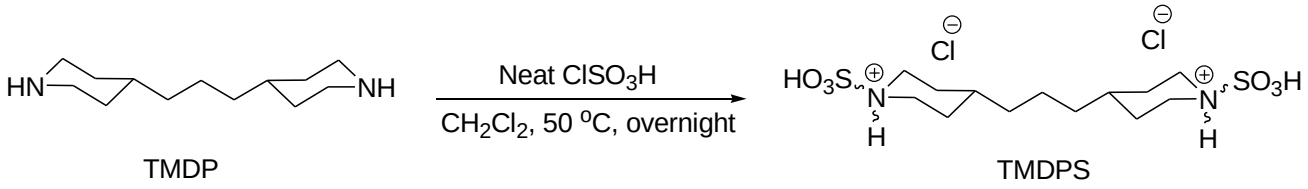

Scheme 1. Synthesis of 4,4'-trimethylene-*N*,*N*'-sulfonic acid-dipiperidinium chloride [TMDPS].

FTIR spectrum of TMDPS is presented in Fig. 1 (see Fig. 1 in Supplementary Material). The broad absorption centered at range 3391 cm^{-1} is assigned to hydrogen bonds of the hydroxyl groups and quaternary ammonium probably corresponding to O–H and NH^+ stretching vibration along with the moisture absorbed by TMDPS. The band at 3035 cm^{-1} probably corresponds to the $N^+H\cdots O$ stretching vibration [47] and the C–H stretching vibrations were observed at 2928 cm^{-1}, and 2851 cm^{-1} [48,49]. Two well defined IR bands were observed in the regions 2520 cm^{-1} and 1622 cm^{-1} which could be arisen from proton tunneling and Fermi resonance interactions with the overtones/combinations of hydrogen-bonded OH bending modes in a strongly hydrogen bonded system with $>NH^+–O_2S–OH$ grouping [50]. The band appeared at the region 2520 cm^{-1} and 1622 cm^{-1} were assigned to the NH^+ stretching band and NH^+ deformation vibration of quaternary ammonium, respectively [47,51].

The identification of C–N stretching frequency is a difficult task since the mixing of bands is possible in this region; hence, the IR band at 1455 cm^{-1} have been designated to C–N stretching modes of vibrations [52]. The asymmetric and symmetric vibrations of SO_2 were observed at range 1300-1000 cm^{-1} [50]. The sharp peaks at 1283 cm^{-1}, 1174 cm^{-1}, and 1044 cm^{-1} can be assigned to the C–N stretching vibration of piperidine ring and S–O bend of sulfonic groups, respectively. The S–N stretching vibration was observed in the region 955 cm^{-1} and 865 cm^{-1} as a series of the medium intensity bands [46]. The bands at 734 cm^{-1} and 581 cm^{-1} have been designated to ring deformation out-of-plane-bending. The C–H out-of-plane-bending peak and the C–H in plane-bending were observed at 734 cm^{-1} [53]. The presence of νS-O(H) as a sharp band and the δNH modes confimed the structure $>NH^+–SO_2–OH$ for TMDPS.

In ^1H NMR spectrum of TMDPS, the acidic hydrogen of sulfonic acid moieties gave two broadened singlets centered at 8.74, 8.73 ppm and NH^+ appeared as one apparent doublet at 8.48 ppm with a large coupling constant 11.4 Hz. Their chemical shifts indicate that these hydrogens were less involved in H-bonding in DMSO-d_6 (see Fig. 2 in Supplementary Material). According to the analysis of chemical shifts and coupling constants (*vide infra*), the piperidinium cation of the TMDPS assumes a chair conformation and the sulfonic acid groups and protons of NH^+ are in the equatorial and the axial position, respectively [54,55]. Signals in ^1H NMR spectra were assigned based on the cross-peaks in 2D measurements (^1H,^1H-COSY); nevertheless, severe overlapping of several signals prevented their complete assignment and only a few coupling constants could be accurately measured. In piperidinium ring, chemical shifts for equatorial hydrogens are found downfield of the axial counterpart owing to shielding or deshielding, respectively, caused by the magnetic anisotropy of ring bonds for chair conformations [56,57]. Therefore, the equatorial (eq) hydrogens of C-2, C-2', C-6, and C-6' were assigned to a well-resolved doublet at 3.19 ppm with a large coupling constant 12.2 Hz. The resonance of the axial (ax) hydrogen of C-2, C-2', C-6, and C-6' appeared as an apparent quartet at 2.79 ppm with large constant coupling 11.4 and 11.2 Hz due to the geminal and ax-ax couplings to the C-2(eq) and C-3(ax) hydrogens, respectively. The apparent doublet signal at 1.74 ppm was assigned to the H-eq of C-3, C-3', C-5, and C-5' with large constant coupling 13.4 Hz. A broadened multiplet at 1.50-1.43 ppm was attributed to axial position of C-4 and C-4'

protons. The H-ax of C-3, C-3', C-5, and C-5' along with hydrogens of trimethylene moiety were observed at 1.30-1.22 and 1.18-1.14 ppm.

^{13}C NMR spectrum of TMDPS exhibits one signal for each of 13 carbon atoms regarding molecular symmetry with chemical shifts 43.7 ppm for C-2, C-2', C-6, C-6'; 28.8 ppm for C-3, C-3', C-5, C-5'; 35.9 ppm for C-4,C-4' (see Fig. 3 in Supplementary Material). The central and lateral carbons of trimethylene moiety were displayed at 33.2 ppm and 23.0 ppm, respectively.

^{1}H,^{1}H-COSY measurement of TMDPS and the analysis of the coupling pattern showed that signal at 8.48 ppm belonged to NH^+ protons which exhibited a correlation with axial and equatorial hydrogens of C2, C2', C6, C6' at 3.19 ppm and 2.79 ppm, and acid hydrogen of sulfonic acid group at 8,74 ppm and 8.73 ppm, respectively. The acidic protons of N–SO_3H moieties showed a weak correlation with H-ax and H-eq of C2, C2', C6, C6', H-eq of C3, C3', C5, C5', and NH^+ at 3.19 ppm, 2.79 ppm, 1.74 ppm, and 8.48 ppm, respectively (see Fig. 4 and 5 in Supplementary Material).

The hydrogen signals of CH-2,2',6,6'(eq) showed the HMBCs correlation with C-α, C-3, and C-2 at δC 28.74, 33.23, and 43.74 ppm with low, high, and high intensities, respectively. The protons of CH-2,2',6,6'(ax) exhibited the HMBCs correlation with C-α, C-3, at δC 28.74, and 33.23 ppm with low intensity (see Fig. 6 in Supplementary Material). The HMBC correlations of the hydrogen signals of CH-3,3',5,5'(eq) with C-3, C-α, and C-4 were observed at δC 28.74, 33.23, and 35.93 ppm with high, high, and low intensities, respectively. The protons of CH-4,4'(ax) exhibit the HMBC correlations with C-β, C-3, C-4, and C-2 at δC 23.01, 28.74, 35.93, and 43.74 ppm with high intensities.

The hydrogens of CH_2-α, CH_2-β and CH-3,3',5,5'(ax) displayed the HMBC correlations with all carbons in TMDPS; however, no the HMBC correlation was observed with Cα and C-2 at ranges 1.30-1.24 ppm and 1.18-1.14 ppm, respectively. The chemical shifts and the coupling constants are displayed in Table 1 (Scheme 2).

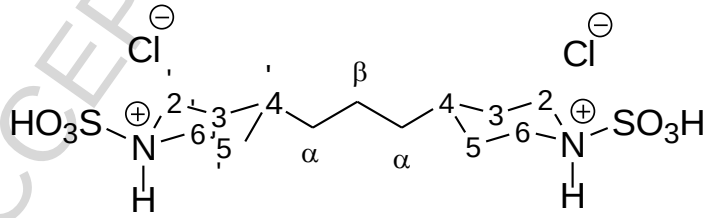

Scheme 2. The elucidated structures of TMDPS based on the 2D NMR experiments.

Table 1. The structure data of TMDPS in DMSO-d_6.

Atom	δH (ppm)	J (Hz)	δC (ppm)
–SO_3H	8.74 and 8.73	br s	-
NH^+	8.48	d, 11.4	-
CH-2, CH-2', CH-6 and CH-6'(eq)	3.19	d, 12.2	43.7
CH-2, CH-2',C H-6 and CH-6'(ax)	2.79	q, 11.4 and 11.2	43.7
CH-3, CH-3', CH-5 and CH-5'(eq)	1.74	d, 13.4	28.74
CH-3, CH-3', CH-5 and CH-5'(ax)	1.30-1.22	m	28.74
CH-4 and CH-4'	1.50-1.43	m	35.93
CH_2-α	1.30-1.22 and 1.18-1.14	m	33.28
CH_2-β	1.30-1.22 and 1.18-1.14	m	23.01

The cations of $C_{13}H_{27}N_2O_6S_2^+$ and $C_{13}H_{27}N_2O_6S_2Na^+$ were detected at m/z 371.13 and 393.12 by positive ion mode LC-ESI-MS for TMDPS.

2.2. The physical properties of TMDPS

TMDPS is a room temperature ionic liquid and showed any signs of crystallization, even well below −4 °C. The density of TMDPS was determined 1.04 g/mL at 27.00 ± 0.02 °C using a Mettler Toledo DM45 Deltarange Density meter. Density measurement of TMDPS was conducted at range 25-90 °C and the temperature dependence of the density for TMDPS is graphically depicted in Fig. 7 (See Supplementary Material). The calibration was performed using doubly distilled and degassed water and dried air at atmospheric pressure.

The viscosity plays a crucial role in a practical and reliable design, analysis, and optimization of processes including mixing, separations, flow chemistry, heat exchangers, pipelines, and distillation columns [58,59]. In most cases, ILs are viscous and their viscosities can be even several orders of magnitude higher than those of water and organic solvents. This unfavorable property is one of the drawbacks to successful applications of ILs in chemical technology and engineering. Therefore, for the future development of ionic liquid science and consequently greener technologies, research on the discovery of new low-viscous ILs is highly demanded.

The viscosity of **TMDPS** was measured 14.1 ± 0.2 mPa s (cP) using a Brookfield DV-III Ultra Viscometer at 27.00 ± 0.02 °C under ambient pressure. The viscosity measurement of TMDPS was performed at range 25-90 °C and the temperature dependence of the viscosity for TMDPS is graphically depicted in Fig. 8 (see Supplementary Material).

The ionic conductivity (σ) of neat TMDPS was measured 1.82 mS cm^{-1} using a Mettler Toledo Seven Easy conductivity meter at 25 °C.

The ILs absorb moisture from the atmosphere during storage; therefore, TMDPS was dried before the determination of its total water content. The total water content of TMDPS was determined 0.22 ± 0.02 wt. %. by Karl Fisher (KF) titration using a Metrohm 831 KF coulometer in conditions of ambient humidity and temperature. The conditions of temperature, pressure and drying time were 100 °C, 80 mbar and 12 h, respectively.

The several 0.01 molar solutions of TMDPS was prepared in the deionized water, and the pH readings were recorded 2.1 ± 0.1 using a pH meter F-71, LAQUA-HORIBA Scientific at 27 ± 1°C. The standard deviations were obtained from three replicate determinations on the different three days.

The new ionic liquid TMDPS was soluble in water, methanol, ethanol, acetonitrile, and acetic acid while was immiscible with ethyl acetate, n-hexane, and toluene.

2.3. Thermal stability of TMDPS

The thermal behavior of TMDPS is showed as DSC plot at the temperature range 30-500 °C in Figure 9 (See Supplementary Material). The baseline was shifted in the endothermic direction due to the decreasing heat capacity of the sample. In nitrogen atmosphere, three endothermic peaks centered around 130 °C, 270 °C, and 310 °C were recorded on the DSC curves of TMDPS and no exothermic peak was observed. The first endothermic peak from 82.7 °C to 146.1 °C was attributed to liberate of the adsorbed water and the chemically

bound hydrogen chloride in the TMDPS sample. The DSC profile indicates that the decomposition of TMDPS include two steps which the first step as main stage occurred at 269.9 °C with heat of decomposition 281.61 J g^{-1} (124.87 KJ mol^{-1}) and the second stage began at 293.8 °C with heat of decomposition 21.29 J g^{-1} (9.44 KJ mol^{-1}), while the tailing ended at 312.5 °C.

TGA/DTG curve of TMDPS is presented in Fig. 10 (See Supplementary Material). Four peaks were visible on DTA curve and TMDPS decomposition goes in three stages according to TGA/DTG curve. DTA curve of TMDPS obtained by analysis in nitrogen atmosphere shows a broad peak below 150 °C centered at 59.5 °C which were attributed to elimination of inherent moisture and physically adsorbed water as well as the chemically bound hydrogen chloride in TMDPS. The first onset of temperature decomposition of TMDPS was observed at 262.05 °C, and its thermal decomposition ended at 262.96 °C which was very compatible to the DSC result. The second and third stages of decomposition were display at 289.45 °C and 433.59 °C, respectively. The maximum mass loss was 98.54% that was related to the total decomposition of piperidine and sulfonic acid fragments of TMDPS. At 263-434 °C, the decomposition of TMDPS was practically completed. The thermal stability of ionic liquids plays very important role when their reactions need to perform at high temperature. All the preceding results showed that TMDPS is thermally stable even at relatively high temperatures and its thermal stability could be a consequence of the presence of hydrogen bonds and electrostatic interactions between $–NH^+$ and $–SO_3H$ groups in the TMDPS.

*2.4. Synthesis of pyrano[4,3-b]pyrans in the presence of **TMDPS***

Initially, the optimum reaction conditions were investigated using the condensation of 4-chlorobenzaldehyde (**1a**), 4-hydroxy-6-methyl-2-pyrone (**A**), and malononitrile as a model reaction (Scheme 3).

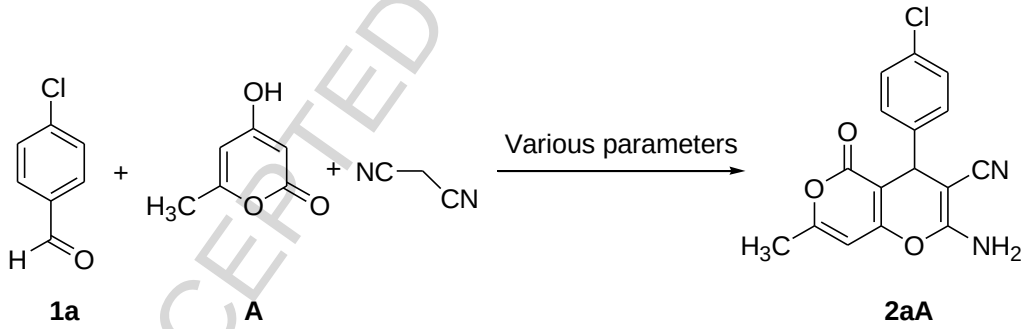

1a **A** **2aA**

Scheme 3. The study of optimal reaction parameters and conditions.

The model reactants were ground at room temperature using a planetary ball mill in the absence of a catalyst under solvent-free conditions. The 2-Amino-4-(4-chlorophenyl)-7-methyl-5-oxo-4*H*,5*H*-pyrano[4,3-*b*]pyran-3-carbonitrile (**2Aa**) was not observed after 4 h (monitored by GC-MS) (Table 2, entry 1). Then, TMDPS was added to the model reactants and the reaction mixture was milled at room temperature for 4 h. The deionized water was added to the mixture and TMDPS was washed from the grinding jar, then the desired product was separated by simple filtration. The ionic liquid was recovered through the evaporation of the water and used for the next run. The residue was washed from the grinding jar with hot ethanol and **2Aa** was obtained in 86% yield after crystallization (Table 2, entry 2). No significant difference in yield was observed when the reaction time was curtailed to 1 h (Table 2, entry 3). The yield dropped to 65%

when the reaction time was reduced to 30 min (Table 2, entry 4). Decreasing the SAIL loading to 5 mol% led to only a slight drop in yield **2Aa** (Table 1, entries 5 and 6) while more decreasing the SAIL loading to as low as 2 mol% decreased yield to 55% (Table 2, entry 7).

Then, the influence of technical parameters such as revolution per minute (r.p.m.), size and number of ball mill on performing the model reaction investigated. The results displayed that the r.p.m. has a crucial influence on the yield of the desired product and the best yield of **2Aa** obtained at 600 rpm after 30 min (Table 2, entries 8-12). At entry 8-10, the milling time was screened to find the optimal milling time while other parameters were kept constant. As shown in Table 2, the decrease of milling time to 30 min led to no drop in yield of **2Aa**. The shorter milling time led to a significant drop in yield of the desired product (Table 2, entry 10).

The size and the number of milling balls were changed while other parameters kept constant. As expected, a higher yield of **2Aa** was observed when experiments were carried out with a larger size and higher number of balls (Table 2, entries 13 and 14). As reported in the literature, these parameters directly influence the active surface area and the total mass of the milling balls [60].

Table 2. Optimization of the synthesis of pyrano[4,3-*b*]pyrans under a variety of reaction conditions.[a]

Entry	Loading **TMDPS** (mol%)	Number of ball mill	Speed (rpm)	Ball mill diameter (mm)	Milling time (min)	Yield (%)[b]
1	0	4	300	7	240	-[c]
2	20	4	300	7	240	86
3	20	4	300	7	60	84
4	20	4	300	7	30	65
5	10	4	300	7	60	84
6	5	4	300	7	60	82
7	2	4	300	7	60	55
8	5	4	600	7	60	92
9	**5**	**4**	**600**	**7**	**30**	**92**
10	5	4	600	7	20	76
11	5	4	500	7	30	88
12	5	4	400	7	30	67
13	5	4	600	5	30	48
14	5	2	600	7	30	46

[a] Reaction conditions: 4-chlorobenzaldehyde (**1a**) (1.0 mmol), 4-hydroxy-6-methyl-2-pyrone (**A**) (1.0 mmol), malononitrile (1.0 mmol), room temperature.

[b] Isolated yield.

[c] Monitored by GC-MS.

The scope and generality of the present protocol for the preparation of pyrano[4,3-*b*]pyran derivatives was evaluated through the condensation of various aldehydes **1**(**a**-**o**), 4-hydroxy-6-methyl-2-pyrone (**A**), and malononitrile under optimized reaction conditions based on entry 9 in Table 2 (Scheme 4).

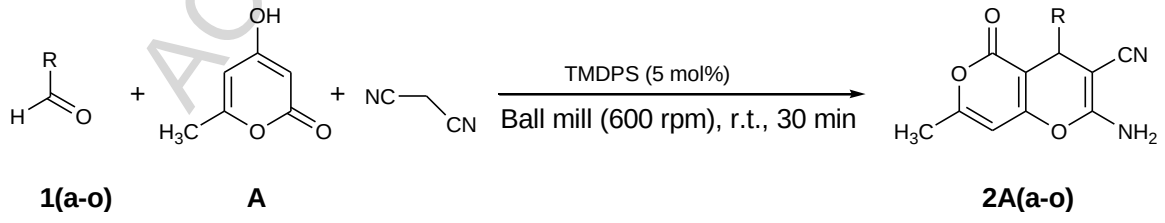

1(a-o) **A** **2A(a-o)**

Scheme 4. Synthesis of pyrano[4,3-*b*]pyran derivatives in the presence of **TMDPS** under optimal conditions.

The aldehydes bearing electron withdrawing and electron donating substituents gave the desired pyrano[4,3-*b*]pyran in good to excellent yields (Table 3). Aldehydes bearing electron withdrawing substituents afforded a slightly higher yield of pyrano[4,3-*b*]pyran than electron donating substituents at same position probably due to increased carbonyl group electrophilic property (Table 3, entries

1,5,12,13 vs 3,4,7). The methoxybenzaldehydes as acid sensitive aldehydes also afforded the desired product in good yield with no decomposition under the optimized reaction conditions (Table 3, entries 7,9,10).

Table 3. The one-pot multicomponent synthesis of pyrano[4,3-*b*]pyran derivatives in the presence of **TMDPS** under optimized reaction conditions.[a]

Entry	Aldehydes **2(a-o)**	Pyrano[4,3-b]pyran **2A(a-o)**	Yield (%)[b]	Melting point (°C)	
				Found	Reported (ref.)
1	4-Cl-C_6H_4-	2Aa	92	219-221	228-230 (61)
2	C_6H_5-	2Ab	85	246-248	236 (61)
3	4-CH_3-C_6H_4-	2Ac	88	226-228	218-220 (61)
4	4-$(CH_3)_2$CH-C_6H_4-	2Ad	86	220-222	-
5	4-NO_2-C_6H_4-	2Ae	92	216-218	220-222 (61)
6	3,5-Cl_2-C_6H_4-	2Af	87	212-214	-
7	4-(CH_3O)-C_6H_4-	2Ag	90	205-207	210-212 (39)
8	2-Cl-C_6H_4-	2Ah	89	258-260	270-272 (62)
9	2-(CH_3O)-C_6H_4-	2Ai	84	242-244	-
10	3,4,5-$(CH_3O)_3$-C_6H_2-	2Aj	82	227-229	235-237 (62)
11	4-Br-C_6H_4-	2Ak	90	219-221	217-219 (39)
12	4-CF_3-C_6H_4-	2Al	91	217-219	-
13	4-F-C_6H_4-	2Am	92	220-222	223-225 (24)
14	3,5-F_2-C_6H_3-	2An	89	240-241	-
15	3,5-$(CF_3)_2$-C_6H_4-	2Ao	92	245-247	-

[a] Reaction conditions: aldehyde **1**(**a-o**) (1.0 mmol), hydroxy-6-methyl-2-pyrone (**A**) (1.0 mmol), malononitrile (1.0 mmol), TMDPS (0.05 mmol), four ball mill with diameter 7 mm, revolution rate (600 rpm), room temperature, milling time (30 min).

[b] Isolated yield.

In continue of the promising catalytic efficiency of TMDPS, we encouraged to evaluate its catalytic performance towards the synthesis of dihydropyrano[3,2-*c*]chromene derivatives and tetrahydrobenzo[*b*]pyrans under the aforementioned optimal reaction conditions. For this goal, the various aryl aldehydes with electron withdrawing and electron releasing groups **1**(**a-l**) and malononitrile were subjected to the reaction with 4-hydroxycoumarin (**B**) and dimedone (**C**). The dihydropyrano[3,2-*c*]chromenes (Scheme 5, Table 4) and tetrahydrobenzo[*b*]pyran derivatives (Scheme 6, Table 5) were obtained in good to excellent yields at room temperature at 600 rpm under solvent-free conditions after 30 min milling time.

1(a-l) **B** **2B(a-l)**

Scheme 5. Synthesis of dihydropyrano[3,2-*c*]chromene derivatives in the presence of TMDPS under optimal reaction conditions.

Table 4. The one-pot multicomponent synthesis of dihydropyrano[3,2-*c*]chromene derivatives in the presence of TMDPS under optimized reaction conditions.[a]

Entry	Aldehydes **2(a-n)**	Dihydropyrano[3,2-*c*]chromene **2B(a-l)**	Yield (%)[b]	Melting point (°C)	
				Found	Reported (ref.)
1	4-Cl-C_6H_4-	2Ba	94	262-264	265-266 (63)
2	C_6H_5-	2Bb	84	254-256	248-250 (63)
3	4-CH_3-C_6H_4-	2Bc	87	249-251	254-255 (63)
4	4-(CH_3O)-C_6H_4-	2Bd	85	242-244	237-239 (64)
5	4-NO_2-C_6H_4-	2Be	92	259-261	250-252 (64)
6	4-OH-C_6H_4-	2Bf	88	261-263	265-267 (64)
7	4-$(CH_3)_2$CH-C_6H_4-	2Bg	91	244-245	251-253 (65)
8	2-Cl-C_6H_4-	2Bh	88	266-268	262-265 (66)
9	2-NO_2-C_6H_4-	2Bi	96	258-259	257-259 (67)
10	3,4,5-$(CH_3O)_3$-C_6H_2-	2Bj	85	269-271	275-277 (68)
11	4-Br-C_6H_4-	2Bk	92	228-230	252-254 (69)
12	4-CF_3-C_6H_4-	2Bl	92	248-250	252-254 (65)

[a] Reaction conditions: aldehyde **1(a-l)** (1.0 mmol), 4-hydroxycoumarin (**B**) (1.0 mmol), malononitrile (1.0 mmol), TMDPS (0.05 mmol), four ball mill with diameter 7 mm, revolution rate (600 rpm), room temperature, milling time (30 min).

[b] Isolated yield.

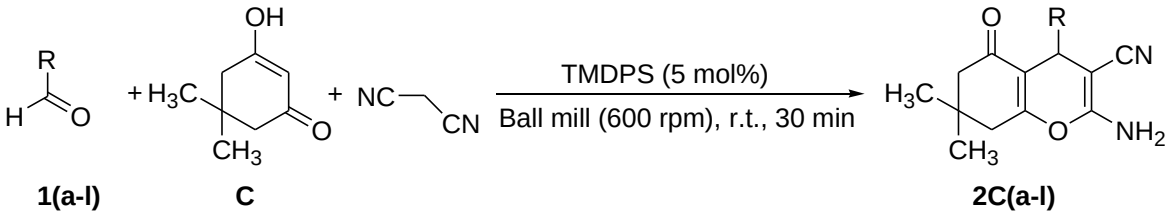

1(a-l) **C** **2C(a-l)**

Scheme 6. Synthesis of tetrahydrobenzo[*b*]pyran derivatives in the presence of TMDPS under optimal reaction conditions.

Table 5. The one-pot multicomponent synthesis of tetrahydrobenzo[*b*]pyran derivatives in the presence of TMDPS under optimized reaction conditions.[a]

Entry	Aldehydes **2(a-n)**	Tetrahydrobenzo[*b*]pyran **2C(a-l)**	Yield (%)[b]	Melting point (°C)	
				Found	Reported (ref.)
1	4-Cl-C_6H_4-	2Ca	96	214-216	215-216 (63)
2	C_6H_5-	2Cb	92	224-226	225-226 (63)
3	4-CH_3-C_6H_4-	2Cc	88	205-207	211-212 (63)
4	4-(CH_3O)-C_6H_4-	2Cd	85	197-199	200-201 (63)
5	4-NO_2-C_6H_4-	2Ce	96	182-184	185-186 (63)
6	4-HO-C_6H_4-	2Cf	90	204-206	206-208 (70)
7	4-$CH_3(CH_2)_4O$-C_6H_4-	2Cg	90	178-180	177-178 (63)
8	2-Cl-C_6H_4-	2Ch	89	215-217	216-217 (63)
9	2-(CH_3O)-C_6H_4-	2Ci	88	198-200	200-201 (63)
10	3,4,5-$(CH_3O)_3$-C_6H_2-	2Cj	85	200-202	208-210 (65)
11	4-Br-C_6H_4-	2Ck	94	197-199	205-207 (65)
12	4-CF_3-C_6H_4-	2Cl	96	217-219	218-219 (63)

[a] Reaction conditions: aldehyde **1(a-l)** (1.0 mmol), dimedone (**C**) (1.0 mmol), malononitrile (1.0 mmol), **TMDPS** (0.05 mmol), four ball mill with diameter 7 mm, revolution rate (600 rpm), room temperature, milling time (30 min).

[b] Isolated yield.

The results of experiments on the synthesis of pyrano[4,3-*b*]pyrans, dihydropyrano[3,2-*c*]chromenes, and tetrahydrobenzo[*b*]pyrans exhibits that TMDPS can be an efficient sulfonic acid-functionalized ionic liquid catalyst for the multicomponent reactions.

A possible mechanism is illustrated in scheme 7. Initially, the aldehyde and 1,3-diketone are activated by TMDPS to promote the reaction. A nucleophilic attack from 1,3-diketone to activated aldehyde provide intermediate (**I**). TMDPS can act as an efficient dehydrating agent and help the dehydration of the intermediate (**I**) [71] which give Knoevenagel intermediate (**II**). In the next step, the knoevenagel intermediate (**II**) reacts with the activated malononitrile by anion part of TMDPS as a Michael acceptor which produces the intermediate (**III**). Then, an intramolecular nucleophilic attack from the oxygen atom to nitrile group followed by tautomerization will give the desired product.

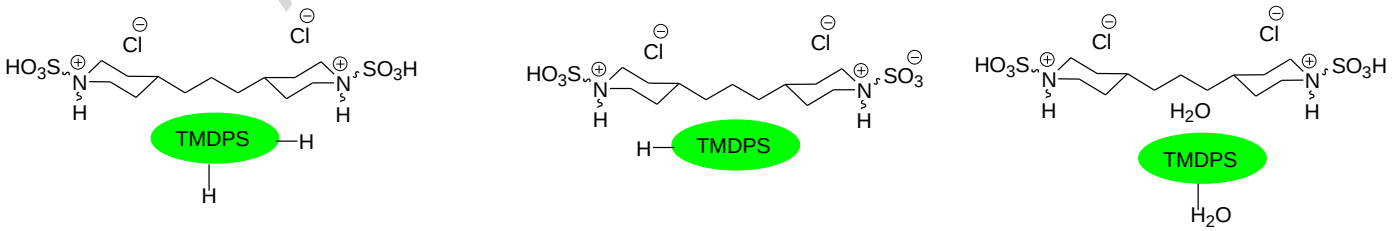

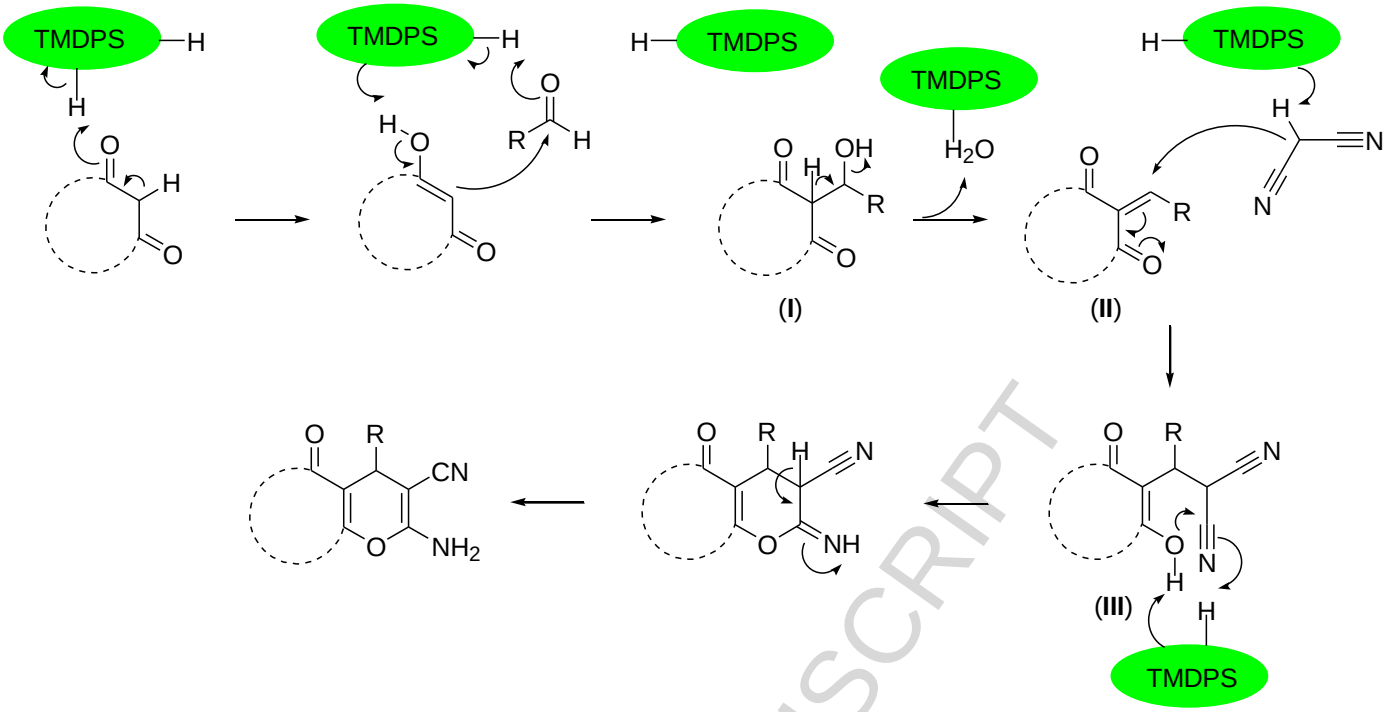

Scheme 7. A possible mechanism illustrated for the one-pot multicomponent reactions in the presence of TMDPS.

This current method was compared with the methods reported in the literature as shown in Tables 6-8. Each of these methods has its advantages, while some still have one or more limitations and drawbacks such as tedious procedures in the preparation of catalyst and separation product/catalyst in the work up step, use of the expensive catalysts or catalysts containing metal/transition metal, conduct the reactions at high temperature for the long reaction time along with a low yield of products, un-recyclability of catalyst, generate the metal wastes, a high catalyst loading, etc.

For example, **2Aa, 2Bb**, and **2Cd** were obtained in 93%, 81%, and 87% yield in the presence of 10 mol% urea at room temperature in aqueous ethanol after 7 h, 3 h, and 9 h, respectively [65]; whereas, the same products were afforded in 92%, 84%, and 85% yield under optimized reaction conditions *via* the current method (Table 6,7, and 8).

The **2Aa** was obtained in 77% yield in the presence of 1 mol% of 1,1,3,3-N,N,N',N'-tetramethylguanidinium trifluoroacetate (TMGT) at 100 °C within 60 min [66], while the identical product was isolated in 85% yield at room temperature after 30 min by the new methodology.

Also, the product **2Aa** was afforded in 89.2% yield within 10 h in the presence of 120 unit of porcine pancreas lipase at room temperature [72], whereas the same reaction gave a 90% yield for **2Aa** at room temperature in the presence of 10 mol% TMDPS after 30 min milling time under solvent-free conditions.

The commercially available catalysts such as thiourea dioxide (formamidinesulfinic acid) (Table 6, entry 4) and piperidine (Table 6, entry 5) requires safe handling and storage due to their self-heating, highly flammablility, and toxicity, respectively [31,36]. Furthermore , the model reactants were ground using mortar and pestle in the presence of NH_4OAc (10 mol%) at room temperature for 14 min [28] which afforded **2Aa** in 32% yield. The desired product **2Aa** was isolated in 54% yield after workup when the identical reaction was

carried out under optimal conditions of the current protocol *viz*. NH_4OAc (5 mol%), room temperature, speed of ball milling (600 rpm), milling time (30 min).

Table 6. The comparison of the present protocol with other reported strategies for the synthesis of 2-amino-4-phenyl-7-methyl-5-oxo-4*H*,5*H*-pyrano[4,3-*b*]pyran-3-carbonitrile.

Entry	Catalyst	Catalyst loading (mol%)	Conditions	Time (min)	Yield (%)	Ref.
1	[BMIM][BF_4]	664	80 °C	180	85	24
2	[NH4][OAc]	10	Solvent-free, grinding, r.t.	10	94	28
3	KF-Al_2O_3	100 mg per 2.0 mmol 4-chlorobenzaldehyde	EtOH, reflux	480[a]	76[a]	29
4	Piperidine	1-2 drops per 1.0 mmol benzaldehyde	MeOH, reflux	60	79	31
5	Thiourea dioxide	10	H_2O, 80 °C	40	92	36
6	4-(Succinimido)-1-butane sulfonic acid	4.2	Neat, 60 °C	60	88	37
7	[BBMIm][HSO_4]	120.5	Solvent-free, 60 °C	35	94	39
8	Succinimide-*N*-sulfonic acid	10	Solvent-free, 60 °C (Solar energy)	35	94	61
9	Urea	10	EtOH:H_2O (1:1 v/v), r.t.	420	81	65
10	TMGT	1.0	Solvent-free, 100 °C	60	77	66
11	Porcine pancreas lipase	120 U	*i*-Propanol, 60 °C	600	89	72
12	-	-	H_2O, 80 °C	630	65	73
13	TMDPS	5	Ball milling, r.t.	30	85	This work

[a]2-Amino-4-(4-chlorophenyl)-7-methyl-5-oxo-4*H*,5*H*-pyrano[4,3-*b*]pyran-3-carbonitrile.

Abbreviative: TMGT = 1,1,3,3-N,N,N',N'-tetramethylguanidinium trifluoroacetate

The product **2Bf** was produced in 88% yield at 100 °C after 34 min in the presence of 6 mg bisferrocene-containing ionic liquid supported on silica coated Fe_3O_4 per mmol of reactants [69], while **2Bf** was isolated in 88% yield at room temperature after 30 min the by the current protocol (Table 7, entry 1). In addition, Fe_3O_4@-SiO_2@imidazol-bisFc[HCO_3] was prepared through a tedious and multi-step process and the aggregation can cause the rapid loss of catalytic activity.

The product **2Ba** was obtained in 94% yield within 5 min in the presence of 20 mol% of DMAP and ethanol under reflux conditions [74], whereas the same reaction in the presence of 5 mol% TMDPS gave 94% yield after 30 min milling time at room temperature under solvent-free conditions (Table 7, entry 7).

In comparison with other catalysts such as DBU [33], urea [65], tetrabutylammonium bromide [75], Diammonium hydrogen phosphate and S-proline [76], Potassium phthalimide-N-oxyl [77], $H_6P_2W_{18}O_{62}$•$18H_2O$ [79], and triethylenetetraammonium trifluoroacetate [81] which were reported in the synthesis of **2Ba**, TMDPS shows more catalytic efficiency in terms of reaction time, catalyst loading, use of solvent, or temperature (Table 7, entries 1,2,6-8, 10,12).

Table 7. The comparison of the present protocol with other reported strategies for the synthesis of 2-amino-4-phenyl-5-oxo-4*H*,5*H*-pyrano[3,2-*c*]chromene-3-carbonitrile.

Entry	Catalyst	Catalyst loading (mol%)	Conditions	Time (min)	Yield (%)	Ref.
1	DBU	10	H_2O, reflux	7	92	33
2	Urea	10	EtOH:H_2O (1:1 v/v), r.t.	360	91	65
3	Fe_3O_4@SiO_2@imidazol-bisFc[HCO_3]	6 mg	Solvent-free, 100 °C	23	87	69
4	Starch solution	4 mL per mmol of aldehyde	Starch solution, 50 °C	25	95	70
5	DMAP	20	EtOH, reflux	5	94[a]	74
6	Tetrabutylammonium bromide	10	H_2O, reflux	45	91	75
			Solvent-free, 120 °C	44	88	
7	Diammonium hydrogen phosphate	10	EtOH:H_2O (1:1 v/v), r.t.	240	81	76
	S-proline	10	EtOH:H_2O (1:1 v/v), reflux	180	72	
8	Potassium phthalimide-N-oxyl	5	H_2O, reflux	12	97	77
9	Zinc ferrite	40 mg per mmol aldehyde	H_2O, 30 °C	180	93	78
10	$H_6P_2W_{18}O_{62}$•$18H_2O$	1	EtOH:H_2O (1:1 v/v), reflux	30	89	79
11	Amberlyst A21	30 mg per 1 mmol aryl aldehyde	EtOH, r.t.	90	87	80
12	[TETA][TFA]	5	EtOH:H_2O (1:1 v/v), reflux	20	86	81
13	TMDPS	5	Ball milling, r.t.	30	84	This work

[a] Aryl aldehyde was 4-chlorobenzaldehyde

Abbreviates: Fe_3O_4@SiO_2@imidazol-bisFc[HCO_3] = Nanomagnetic bisferrocene-containing ionic liquid supported on silica coated Fe_3O_4; DBU = 1,8-Diazabicyclo[5.4.0]undec-7-ene; DMAP = 4-(dimethylamino)pyridine; [TETA][TFA] = triethylenetetraammonium trifluoroacetate

In comparison with the reported catalysts such as urea [65], 2,2,2-trifluoroethanol [82], and [BMIM]Br [83] for the synthesis of 2-amino-7,7-dimethyl-5-oxo-4-phenyl-5,6,7,8-tetrahydro-4H-benzopyran-3-carbonitrile (**2Cb**), our protocol showed the comparative yields at shorter reaction time (Table 8). Furthermore, this current methodology showed superiority to the reported reports such as DMAP [74], Potassium phthalimide-N-oxyl [77], triethylenetetraammonium trifluoroacetate [81], 2,2,2-trifluoroethanol [82], Phenylboronic acid [84], Thiamine hydrochloride [86], and [H_2-DABCO][H_2PO_4]$_2$ [87] in term of the reaction temperature.

The reaction catalyzed by 28 mol% taurine (2-aminoethanesulfonic acid) in water afforded **2Cb** in 82% yield under reflux conditions after 65 min [88], while the **2Cb** was obtained in 84% yield under optimal conditions by new developed methodology (Table 8, entry 12). In addition, the **2Cd** was afforded in 78% yield in the presence of Amberlyst A21 (30 mg per mmol aldehyde) in ethanol at room temperature after 90 min [80], and the **2Cd** was isolated in 85% yield after 30 min milling time at room temperature using the new protocol under solvent-free conditions.

Table 8. The comparison of the present protocol with other reported strategies for the synthesis of 2-amino-7,7-dimethyl-5-oxo-4-phenyl-5,6,7,8-tetrahydro-4*H*-benzopyran-3-carbonitrile.

Entry	Catalyst	Catalyst loading/mol%	Conditions	Time/min	Yield/%	Ref.
1	Urea	10	EtOH:H_2O (1:1 v/v), r.t.	360	91	65
2	DMAP	20	EtOH, reflux	15[a]	94[a]	74
3	Potassium phthalimide-N-oxyl	5	H_2O, reflux	15	95	77
4	Amberlyst A21	30 mg per mmol aldehyde	EtOH, r.t.	60	87	80
5	[TETA]TFA	5	EtOH:H_2O (1:1 v/v), reflux	20	85	81
6	2,2,2-Trifluoroethanol	2 mL per mmol of aldehyde	2,2,2-trifluoroethanol, reflux	300	90	82
7	[BMIM]Br	25	EtOH:H_2O (1:1 v/v), r.t.	24-30 h	65-96	83
8	Phenylboronic acid	5	EtOH:H_2O (1:1 v/v), reflux	30	88	84
9	Fructose	20	EtOH:H_2O (1:2 v/v), 40 °C	45	86	85
10	Thiamine hydrochloride (VB1)	10	EtOH, reflux	15	90	86
11	[H_2-DABCO][H_2PO_4]$_2$	16	EtOH:H_2O (2:1 v/v), reflux	12	90	87
12	Taurine (2-aminoethanesulfonic acid)	28	H_2O, reflux	65	82	88
13	TMDPS	5	Ball milling, r.t.	30	92	This work

[a] Aryl aldehyde was 4-chlorobenzaldehyde

Abbreviates: Fe_3O_4@Ph-SO_3H = magnetic iron oxide supported phenylsulfonic acid; [TETA]TFA = Triethylenetetraammonium trifluoroacetate; SiO_2-Pr-SO_3H = silica based sulfonic acid

The feasibility of the present method on gram scaled experiment was investigated through the condensation of 4-chlorobenzaldehyde (10 mmol), malononitrile (10 mmol), and 4-hydroxycoumarin (10 mmol) using 5 mol% TMDPS at room temperature under optimized reaction conditions which afforded the desired product, 2-amino-5-oxo-4-phenyl-4,5-dihydropyrano[3,2-*c*]-chromene-3-carbonitrile (**2Ba**) in 81% isolated yield within 30 min, almost identical in all respects with mmol scale entry.

It is well-known that the chemical structure of the cations and anions determined the physical and chemical properties. In addition, the catalytic activity of ionic liquids is related to the interaction between the functional and acceptor/donner hydrogen bond groups on the cation or anion moieties of ionic liquids with reactants. The chemists often change the chemical structure of ionic liquids through insert new functional groups and investigate the modification effects on their physical and chemical properties as well as their catalytic activity in the model reaction under identical conditions [89]. This process can be one of attempting to understand and reveal how properties

relevant to catalytic activity of ionic liquid are encoded by the chemical structure cation and anion. This can allow the chemist to design and change the structure of cation/anion or functional groups of ILs which lead to new ILs with desired physical and chemical properties and catalytic activities. Herein, the catalytic efficiency of di-cationic ionic liquids containing di-sulfonic groups along with nonacidic (Cl^-) and acidic (HSO_4^-) counter anion was compared with new SAIL to the synthesis of **2Aa, 2Ba** and **2Ca** under aforementioned optimized conditions (Table 9). The sulfonic acid-functionalized imidazolium ionic liquids were prepared according to the literature [46].

Table 9. Comparison of the result obtained for the synthesis of **2Aa**, **2Ba**, and **2Ca** in the presence of some sulfonic-functionalized ionic liquid containing di-cationic nucleus with carbon spacer.[a]

Entry	IL as solvent-catalyst	Abbreviation	Yield (%)[b]		
			2Aa	**2Ba**	**2Ca**
1	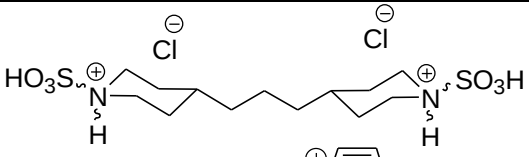	TMDPS	92	94	96
2	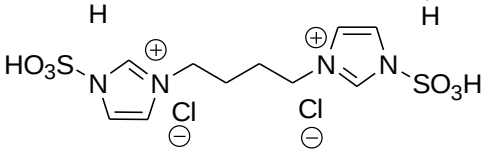	BBSI-Cl	92	93	96
3	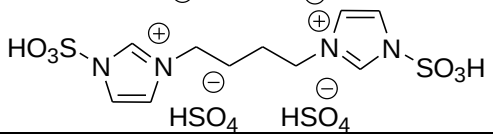	BBSI-HSO_4	98	98	98

[a] Reaction conditions: Reaction conditions: 4-chlorobenzaldehyde **1a** (1.0 mmol), hydroxy-6-methyl-2-pyrone (**A**) (1.0 mmol) or dimedone (**B**) or dimedone (**C**), malononitrile (1.0 mmol), IL (0.05 mmol), four ball mill with diameter 7 mm, revolution rate (600 rpm), room temperature, milling time (30 min), solvent-free conditions.

[b]Isolated yield.

As shown in Table 9, the best result was obtained with the BBSI-HSO_4 while a slightly drop of the catalytic efficiency was observed with BBSI-Cl and TMDPS. TMDPS and BBSI-Cl showed the same catalytic efficiency; therefore, it seems that the C2-H of imidazole ring does not play an important role in the promotion of the reaction when the sulfonic acid groups are present (Table 9, entries 1 and 2). Also, the results showed that sulfonic acid-functionalized IL containing acidic anion such as HSO_4^- is more efficient than that with a non-acidic anion such as Cl^- (Table 9, entries 2 and 3).

2.5. Reusability of TMDPS

On completion of the reaction, the desired products were readily extracted using hot ethyl acetate, and the remained SAIL was concentrated under reduced pressure. Then, the reaction jar was recharged with new model reactants for another run. During three subsequent runs, a range 92-90%, 94-90%, and 96-94% yield were obtained for **2Aa, 2Ba**, and **2Ca** in the presence of TMDPS, respectively. Furthermore, the chemical structure of TMDPS showed no significant change under the present workup (See Fig. 11 in Supplementary Material).

Also, the ionic liquid could be separated by washing with deionized water followed by evaporation of water from an aqueous solution containing TMDPS. The recovered ionic liquid was successfully reused for the subsequent runs without significant loss of catalytic

activity. Therefore, either the isolation of product or the separation of ionic liquid was practical for the recovering of TMDPS after reactions.

3. Experiment

3.1. General

Unless specified, all chemicals were analytical grade and purchased from Merck, Aldrich, and Fluka Chemical Companies and used without further purification. Products were characterized by their physical constant and IR, NMR and elemental analysis. The purity determination of the substrates and reaction monitoring were accompanied by TLC using silica gel SIL G/UV 254 plates. The FT-IR spectra were recorded on a Perkin Elmer 781 Spectrophotometer using KBr pellets for solid and neat for liquid samples in the range of 4000-400 cm^{-1}. In all the cases the ^{1}H and ^{13}C NMR spectra were recorded with Bruker Avance III 600 MHz and 400 MHz instruments. All chemical shifts are quoted in parts per million (ppm) relative to TMS using deuterated solvent. Microanalyses were performed on a Perkin- Elmer 240-B microanalyzer. Melting points were recorded on a Büchi B-545 apparatus in open capillary tubes. The mass spectra of the products were recorded using an Agilent 6560 iFunnel Q–TOF LC–MS instrument. Ball-milling was performed in a Retsch PM100 planetary ball mill using a 25 mL stainless steel chamber and two or four stainless steel balls (diameter: 5 or 7 mm) with 300-600 revolution per minute (rpm).

TGA/DTA curves were obtained with the use of a Mettler Toledo TGA/SDTA 851e. All measurements were taken in the Al_2O_3 crucible with the sample mass 10.02 mg under nitrogen atmosphere (30 mL min^{-1}). Dynamic scans were performed at the heating rate of 10 °C min^{-1} in the temperature range 30–800 °C.

Differential scanning calorimetry (DSC) curves were obtained with the use of a DSC-Mettler Toledo DSC 822e calorimeter. The measurements were taken in the aluminum pans with a pierced lid with the sample mass 17.01 mg under a dry nitrogen gas atmosphere (30 mL min^{-1}). Dynamic scans were performed at a heating rate of 10 °C min^{-1} in the temperature range 30–500 °C.

3.2. The synthesis of 4,4'-trimethylene-N,N'-sulfonic acid-dipiperidinium chloride [TMDPS]

The neat chlorosulfonic acid (3.0 mL, 40 mmol) was dropwise added to 4,4'-trimethylene-dipiperidine (4.21 g, 20 mmol) in dry CH_2Cl_2 (20 mL). The reaction mixture was stirred at 50 °C for overnight which led to the formation of two phases. The upper phase was decanted, and excess of solvent was removed under reduced pressure. The resulting ionic liquid was isolated as a low-viscous pale yellow liquid which its structure was characterized by FTIR, Mass spectra, 1D and 2D NMRs.

3.3. *Typical procedure for the synthesis of pyran-annulated derivatives in the presence of TMDPS*

The aldehyde (1.0 mmol), malononitrile (1.0 mmol), active methylene compounds (1.0 mmol) [hydroxy-6-methyl-2-pyrone (**A**), 4-hydroxycoumarin (**B**) or dimedone (**C**)], TMDPS (5 mol %) were ground vigorously using the planetary ball mill at room temperature for 30 min. The progress of the reaction was monitored by TLC. On completion of the reaction, the product was extracted by hot ethyl acetate which after evaporation of the solvent, the solid crude product was purified just by recrystallization from ethanol without tedious column chromatographic purification. The TMDPS was concentrated under reduced pressure, and the reaction jar was recharged with

new reactants for another reaction. The structure of each purified 4*H*-pyran-annulated heterocyclic scaffolds was confirmed by melting point and spectral studies including FT-IR, ^{1}H NMR, ^{13}C NMR, and elemental analysis. All the known compounds had physical and spectroscopic data identical to the literature data.

3.4. Physical and spectral data of new products

*2-Amino-4-(4-isopropylphenyl)-7-methyl-5-oxo-4H,5H-pyrano[4,3-b]pyran-3-carbonitrile (**2Ad**)*: m.p. 220-222 °C; FT-IR (KBr) ν_{max} = 3365, 3300, 2200, 1715, 1670, 1640, 1615, 1375, 1265 cm^{-1}; ^{1}HNMR (400 MHz, DMSO-d_6) δ = 7.20-7.18 (m, 3H), 7.10 (d, 2H, *J* = 8.8 Hz), 6.28 (s, 1H), 4.25 (s, 1H), 2.85 (s, 1H), 2.21 (s, 3H), 1.20 (s, 3H), 1.18 (s, 3H) ppm; ^{13}C NMR (100 MHz, DMSO-d_6) δ = 163.1, 161.7, 158.5, 158.4, 147.3, 141.3, 127.7, 126.7, 119.8, 101.2, 98.2, 58.3, 36.1, 33.3, 24.1, 24.2, 19.6 ppm; Anal. Calcd. for $C_{19}H_{18}N_2O_3$: C, 70.79; H, 5.63; N, 8.69. Found: C, 70.73; H, 5.68; N, 8.74.

*2-Amino-4-(3,5-dichlorophenyl)-7-methyl-5-oxo-4H,5H-pyrano[4,3-b]pyran-3-carbonitrile (**2Af**)*: m.p. 212-214 °C; FT-IR (KBr) ν_{max} = 3404, 3330, 2194, 1708, 1676, 1645, 1615, 1382, 1262 cm^{-1}; ^{1}HNMR (400 MHz, DMSO-d_6) δ = 7.46 (t, *J* =1.8 Hz, 1H), 7.20-7.18 (m, 2H), 6.98 (s, 2H), 6.30 (s, 1H), 4.46 (s, 1H), 2.28 (s, 3H) ppm; ^{13}C NMR (100 MHz, DMSO-d_6) δ = 164.1, 162.0, 160.8, 158.7, 145.7, 134.6, 127.4, 122.5, 117.3,104.0, 98.4, 56.3, 39.5, 19.6 ppm; Anal. Calcd. for $C_{16}H_{10}Cl_2N_2O_3$: C, 55.04; H, 2.89; N, 8.02. Found: C, 54.97; H, 2.83; N, 8.04.

*2-Amino-4-(2-methoxyphenyl)-7-methyl-5-oxo-4H,5H-pyrano[4,3-b]pyran-3-carbonitrile (**2Ai**)*: m.p. 242-244 °C; FT-IR (KBr) ν_{max} = 3385, 3295, 2195, 1710, 1676, 1640, 1605, 1380, 1260 cm^{-1}; ^{1}HNMR (400 MHz, DMSO-d_6) δ = 7.20-7.18 (m, 1H), 7.05-6.98 (m, 2H), 6.92-6.87 (m, 3H), 4.70 (s, 1H), 3.68 (s, 3H), 2.30 (s, 3H) ppm; ^{13}C NMR (100 MHz, DMSO-d_6) δ = 164.3, 162.0, 158.8, 158.5, 155.7, 132.6, 130.6, 128.4, 120.5, 118.3, 112.0, 102.9, 98.4, 56.3, 55.7, 35.5, 19.7 ppm; Anal. Calcd. for $C_{17}H_{14}N_2O_4$: C, 65.80; H, 4.55; N, 9.03. Found: C, 65.87; H, 4.61; N, 9.04.

*2-Amino-4-(4-trifluoromethyl-phenyl)-7-methyl-5-oxo-4H,5H-pyrano[4,3-b]pyran-3-carbonitrile (**2Al**)*: m.p. 217-219 °C; FT-IR (KBr) ν_{max} = 3395, 3325, 2190, 1685, 1655, 1370, 1325, 1120 cm^{-1}; ^{1}HNMR (400 MHz, DMSO-d_6) δ = 7.70 (d, *J* = 8.4 Hz, 2H), 7.51 (s, 2H), 7.46 (d, *J* = 8.4 Hz, 2H), 4.58 (s, 1H), 2.91 (s, 3H) ppm; ^{13}C NMR (100 MHz, DMSO-d_6) δ = 163.8, 162.4, 159.0, 157.9, 143.8, 134.6 (q, $^{2}J_{C\text{-}F}$ = 28 Hz), 125.6 (q, $^{1}J_{C\text{-}F}$ = 273 Hz), 125.1 (q, $^{3}J_{C\text{-}F}$ = 4 Hz), 118.3, 105.2, 98.4, 55.8, 39.5, 19.8 ppm; Anal. Calcd. for $C_{17}H_{11}F_3N_2O_3$: C, 58.63; H, 3.18; N, 8.04. Found: C, 58.67; H, 3.22; N, 7.99.

*2-Amino-4-(4-fluorophenyl)-7-methyl-5-oxo-4H,5H-pyrano[4,3-b]pyran-3-carbonitrile (**2Am**)*: m.p. 220-222 °C; FT-IR (KBr) ν_{max} = 3398, 3322, 2194, 1688, 1648, 1368, 1329, 1117 cm^{-1}; ^{1}HNMR (400 MHz, DMSO-d_6) δ = 7.25-7.12 (m, 6H), 6.28 (s, 1H), 4.31 (s, 1H), 2.22 (s, 3H) ppm; ^{13}C NMR (100 MHz, DMSO-d_6) δ = 163.4, 161.7 (d, $^{1}J_{C\text{-}F}$ = 267 Hz), 158.6, 158.5, 140.2, 129.9 (d, $^{3}J_{C\text{-}F}$ = 7 Hz), 119.8, 115.6, 115.4 (d, $^{2}J_{C\text{-}F}$ = 26 Hz), 100.9, 98.5, 58.2, 36.1, 19.7 ppm; Anal. Calcd. for $C_{16}H_{11}FN_2O_3$: C, 64.43; H, 3.72; N, 9.39. Found: C, 64.47; H, 3.68; N, 9.34.

*2-Amino-4-(3,5-difluorophenyl)-7-methyl-5-oxo-4H,5H-pyrano[4,3-b]pyran-3-carbonitrile (**2An**)*: m.p. 240-242 °C; FT-IR (KBr) ν_{max} = 3404, 3330, 2194, 1707, 1675, 1644, 1615, 1381, 1261, 1120, 993, 777 cm^{-1}; ^{1}HNMR (400 MHz, DMSO-d_6) δ = 7.33 (s, 2H), 7.16-7.08 (m, 1H), 7.01-6.94 (m, 2H), 6.30 (s, 1H), 4.43 (s, 1H), 2.25 (s, 3H) ppm; ^{13}C NMR (100 MHz, DMSO-d_6) δ = 163.8, 162.8 (dd,

$^{1}J_{C\text{-}F}$ = 244.5 and 12.8 Hz), 161.8, 159.2, 158.7, 148.7 (t, $^{3}J_{C\text{-}F}$ = 8.2 Hz), 119.4, 111.4 (dd, $^{2}J_{C\text{-}F}$ = 24.0 and 7.5 Hz), 103.0 (t, $^{2}J_{C\text{-}F}$ = 25.5 Hz), 99.9, 98.6, 57.3, 36.5, 19.8 ppm; Anal. Calcd. for $C_{16}H_{10}F_2N_2O_3$: C, 60.67; H, 3.19; N, 8.86. Found: C, 60.71; H, 3.18; N, 8.81.

*2-Amino-4-(3,5-bis(trifluoromethyl)phenyl)-7-methyl-5-oxo-4H,5H-pyrano[4,3-b]pyran-3-carbonitrile (**2Ao**)*: m.p. 245-247 °C; FT-IR (KBr) ν_{max} = 3421, 3339, 3210, 2193, 1720, 1674, 1646, 1611, 1384, 1283, 1172, 1125, 980, 904, 706 cm^{-1}; ^{1}HNMR (400 MHz, DMSO-d_6) δ = 8.02 (s, 1H), 7.96 (s, 2H), 7.41 (s, 2H), 6.32 (s, 1H), 4.72 (s, 1H), 2.25 (s, 3H) ppm; ^{13}C NMR (100 MHz, DMSO-d_6) δ = 164.0, 161.9, 159.3, 158.8, 147.3, 130.6 (q, $^{2}J_{C\text{-}F}$ = 32.2 Hz), 129.2, 123.8 (d, $^{1}J_{C\text{-}F}$ = 270.8 Hz), 121.5, 119.4, 99.4, 98.7, 56.8, 36.4, 19.8 ppm; Anal. Calcd. for $C_{18}H_{10}F_6N_2O_3$: C, 51.94; H, 2.42; N, 6.73. Found: C, 51.89; H, 2.38; N, 6.69.

3.5. Physical and spectral data of known products

*2-amino-7-methyl-5-oxo-4-(4-nitrophenyl)-4H,5H-pyrano[4,3-b]pyran-3-carbonitrile (**2Ae**)*: m.p. 216-218 °C; FT-IR (KBr) ν_{max} = 3497, 3316, 3158, 2203, 1705, 1678, 1653, 1622, 1595, 1520 cm^{-1}; ^{1}HNMR (400 MHz, DMSO-d_6) δ = 8.15 (d, *J* = 8.8 Hz, 2H), 7.55 (d, *J* = 8.8 Hz, 2H), 7.33 (s, 2H), 6.30 (s, 1H), 4.49 (s, 1H), 2.22 (s, 3H) ppm.

*2-amino-7-methyl-5-oxo-4-(4-methoxyphenyl)-4H,5H-pyrano[4,3-b]pyran-3-carbonitrile (**2Ag**)*: m.p. 205-207 °C; FT-IR (KBr) ν_{max} = 3455, 3312, 3168, 2186, 1728, 1676, 1646, 1607, 1510 cm^{-1}; ^{1}HNMR (400 MHz, DMSO-d_6) δ = 7.12 (s, 2H), 7.08 (d, *J* = 8.8 Hz, 2H), 6.84 (d, *J* = 8.8 Hz, 2H), 6.24 (s, 1H), 4.21 (s, 1H), 3.71 (s, 3H), 2.20 (s, 3H) ppm.

*2-amino-7-methyl-5-oxo-4-(3,4,5-trimethoxyphenyl)-4H,5H-pyrano[4,3-b]pyran-3-carbonitrile (**2Aj**)*; m.p. 235-237 °C; FT-IR (KBr) ν_{max} = 3118, 1754, 1621, 1565, 1512, 1410, 1230 cm^{-1}; ^{1}HNMR (400 MHz, DMSO-d_6) δ = 7.10 (s, 2H), 6.82 (s, 2H), 6.12 (s, 1H), 4.20 (s, 1H), 3.91 (s, 6H), 3.82 (s , 3H), 2.34 (s, 3H) ppm.

*2-Amino-5-oxo-4-(4-trifluoromethyl-phenyl)-4H,5H-pyrano[3,2-c]chromene-3-carbonitrile (**2Bl**)*: m.p. 208-210 °C; FT-IR (KBr) ν_{max} = 3325, 3194, 3072, 2877, 2198, 1716, 1602, 1377, 1112, 765 cm^{-1}; ^{1}H NMR (400 MHz, DMSO-d_6) δ = 7.91(d, *J* = 7.6 Hz), 7.73 (t, *J* = 7.0 Hz, 1H), 7.68 (d, *J* = 8.6 Hz, 2H), 7.47-7.53 (m, 6H), 4.60 (s, 1H) ppm.

*2-amino-5-oxo-4-(3,4,5-trimethoxyphenyl)-4H,5H-pyrano[3,2-c]chromene-3-carbonitrile (**2Bj**)*: m.p. 208-210 °C; FT-IR (KBr) ν_{max} = 3123, 1765, 1623, 1535, 1524, 1410, 1230 cm^{-1}; ^{1}H NMR (400 MHz, DMSO-d_6) δ = 8.00 (d, *J* = 8.0 Hz, 1H), 7.75-7.70 (m, 1H), 7.65 (d, *J* = 7.6 Hz, 1H), 7.45-7.39 (m, 1H), 7.26 (s, 2H), 6.79 (s, 2H), 4.34 (s, 1H), 3.80 (s, 6H), 3.72 (s , 3H) ppm.

2-Amino-7,7-dimethyl-5-oxo-4-(4-pentyloxy-phenyl)-5,6,7,8-tetrahydro-4*H*-chromene-3-carbonitrile *(**2Cg**)*: m.p. 178-180 °C; FT-IR (KBr) ν_{max} = 3545, 3327, 3215, 2937, 2193, 1683, 1653, 1606, 1508, 1367, 1251, 1211, 1174, 1035, 842 cm^{-1}; ^{1}H NMR (400 MHz, $CDCl_3$) δ = 7.13 (d, *J* = 8.5 Hz, 2H), 6.80 (d, *J* = 8.5 Hz, 2H), 4.49 (s, 2H), 4.35 (s, 1H), 3.90 (t, *J* = 7.0 Hz, 2H), 2.44 (s, 2H), 2.19 and 2.24 (AB system, *J* = 16.5 Hz, 2H), 1.75 (quin, *J* = 7.0 Hz, 2H), 1.33-1.44 (m, 4H), 1.10 (s, 3H), 1.03 (s, 3H), 0.92 (t, *J* = 7.0 Hz, 3H) ppm.

4. Conclusion

In summary, a novel binuclear sulfonic-functionalized ionic liquid was prepared and its structure was characterized by FTIR, ^{1}H and ^{13}C NMR, Mass spectra. The physical properties such as density and viscosity and pH of the aqueous solution of ionic liquid were

determined. The catalytic efficiency of TMDPS was demonstrated for a one-pot multicomponent reaction under mild conditions. The structure-activity relationship (SAR) of the novel binuclear sulfonic-functionalized acid were studied in comparison with some previously reported sulfonic-functionalized ionic liquids which proved the superiority of binuclear ionic liquids containing sulfonic-functionalized imidazolium moiety with an acidic counter anion. The current protocol has the advantages such as simple experimental and sustainable procedure, high yield of the desired products within short reaction times, a broad substrate scope, and recyclability of novel ionic liquid. The application of TMDPS in the one-pot multicomponent reactions has highlighted the importance of binuclear sulfonic acid-functionalized ionic liquids as an efficient and recyclable catalyst in organic chemistry, and we hope that our work will encourage further research in this area with promising results for future applications of TMDPS.

Conflicts of interest

There are no conflicts of interest to declare.

Acknowledgments

The authors are grateful to staff members in the Analytical and Testing Center of Malaya University for partial support.

References

[1] A.S. Amarasekara, Chem. Rev.116 (2016) 6133-6183.

[2] D.D. Patel, J.M. Lee, Chem. Rec. 12 (2012) 329-355.

[3] M. Koel, Crit. Rev. Anal Chem. 35 (2005) 177-192.

[4] X. Sun, H. Luo, S. Dai, Chem. Rev. 112 (2012) 2100-2128.

[5] R. koda-Földes, Molecules 19 (2014) 8840-8884.

[6] H. Olivier-Bourbigou, L. Magna, J. Mol. Catal. A Chem. 182–183 (2002) 419-437.

[7] Z.S. Qureshi, K.M. Deshmukh, B.M. Bhanage, Clean Technol. Envir. 16 (2014) 1487-1513.

[8] M. Bielejewski, M. Ghorbani, M.A. Zolfigol, J. Tritt-Goc, S. Noura, M. Narimani, M. Oftadeh, RSC Adv. RSC Adv. 6 (2016) 108896-108907.

[9] A. Khazaei, M.A. Zolfigol, A.R. Moosavi-Zare, A. Zare, Sientica Iranica Trans. C Chem. Chem. Eng. 17 (2010) 31-36.

[10] M.A. Zolfigol, A. Khazaei, A.R. Moosavi-Zare, A. Zare, H.G. Kruger, Z. Asgari, V. Khakyzadeh, M. Kazem-Rostami, J. Org. Chem. 77 (2012) 3640-3645.

[11] M. Zarei, E. Noroozizadeh, A.R. Moosavi-Zare, M.A. Zolfigol, J. Org. Chem. 83 (2018) 3645-3650.

[12] M.A. Zolfigol, Tetrahedron 57 (2001) 9509-9511.

[13] N.G Khaligh, T. Mihankhah, Mohd Rafie Johan, Polycycl. Arom. Comp. Doi:10.1080/10406638.2018.1538058.

[14] N. G. Khaligh, Res. Chem. Intermed. 44 (2018) 4045-4062.

[15] J.-L. Do, T. Friščič, ACS Cent. Sci. 3 (2017) 13-19.

[16] M.A.P. Martins, C.P. Frizzo, D.N. Moreira, L. Buriol, P. Machado, Chem. Rev. 109 (2009) 4140-4182

[17] B. Kubias, M.J.G. Fait, R. Schlogl, in Hand book of Heterogeneous Catalysis, ed. Ertl G, Knozinger H, Schuth F, Weitkamp J, Wiley-VCH, Weinheim, 2nd edn, 2008, pp. 571-583.

[18] A.L. Garay, A. Pichon, S.L. James, Chem. Soc. Rev. 36 (2007) 846-855.

[19] N.G. Khaligh, H.S. Abbo, S.J.J. Titinchi, Res. Chem. Intermed. 43 (2017) 901-910.

[20] N.G. Khaligh, O.C. Ling, T. Mihankhah, M.R. Johan, J.J. Ching, Aust. J. Chem. 2018, DIO: 10.1071/CH18408.

[21] A. Stolle, T. Szuppa, S.E.S. Leonhardt, B. Ondruschka, Chem. Soc. Rev. 40 (2011) 2317-2329.

[22] I.V. Magedov, M. Manpadi, M.A. Ogasawara, A.S. Dhawan, S. Rogelj, S. Van slambrouck, W.F.A. Steelant, N.M. Evdokimov, P.Y. Uglinskii, E.M. Elias, E.J. Knee, P. Tongwa, M. Yu. Antipin, A. Kornienko, J. Med. Chem. 51 (2008) 2561-2570.

[23] D. Kumar, P. Sharma, H. Singh, K. Nepali, G.K. Gupta, S.K. Jaina, F. Ntie-Kang, RSC Adv. 7 (2017) 36977-36999.

[24] X. Fan, D. Feng, Y. Qu, X. Zhang , J. Wang , P.M. Loiseau, G. Andrei , R. Snoeck , E. De Clercq, Bioorg. Med. Chem. Lett. 20 (2010) 809-813.

[25] M.D. Aytemir, U. Calis, M. Ozalp, Arch. Pharm. 337 (2004) 281-288.

[26] R.L.T. Parreira, O. Abrahão, S.E. Galembeck. Tetrahedron 57 (2001) 3243-3253.

[27] L. Abrunhosa, M. Costa, F. Areias, A. Venâncio, F. Proenca, J. Ind. Microbiol. Biotechnol. 34 (2007) 787-792.

[28] D. Rajguru, B.S. Keshwal, S. Jain, Med. Chem. Res. 22 (2013) 5934-5939.

[29] X.S. Wang, J.X. Zhou, Z.S. Zeng, Y.-L. Li, D.-Q. Shi, S.-J. Tu, Arkivoc 11 (2006) 107-113.

[30] D.Q. Shi, L.H. Niu, Q.Y. Zhuhang, Chin. J. Org. Chem. 28 (2008) 1633-1636.

[31] E. V. Stoyanov, I.C. Ivanov, D. Heber, Molecules 5 (2000) 19-32.

[32] M. Seifi, H. Sheibani, Catal. Lett. 126 (2008) 275-279.

[33] J.M. Khurana, B. Nand, P. Saluja, Tetrahedron 66 (2010) 5637-5641.

[34] D. Rajguru, B.S. Keshwal, S. Jain, Chin. Chem. Lett. 24 (2013) 1033-1036

[35] E. Mosaddegh, A. Hassankhani, H. Karimi-Maleh, Mater. Sci. Eng., C 46 (2015) 264-269.

[36] M. Ghashang, S.S. Mansoor, K. Aswin, Chin. J. Catal. 35 (2014) 127-133.

[37] N. G. Khaligh, Chin. Chem. Lett. 26 (2015) 26-30.

[38] E. Mosaddegh, A. Hassankhani, Chin. J. Catal. 35 (2014) 351-356.

[39] N.G. Khaligh, Monatsh. Chem. 145 (2014) 1643-1648.

[40] M.N. Elinson, R.F. Nasybullin, G.I. Nikishin, Electrocatalysis 4 (2013) 56-60.

[41] D. Rajguru, B.S. Keshwal, S. Jain, V.W. Bhagwat, Monatsh. Chem. 144 (2013) 1411-1416.

[42] R.N. Rao, M.V.N.K. Talluri, J. Pharmaceut. Biomed. 43 (2007) 1-13.

[43] N.G. Khaligh, Polycycl. Arom. Comp. 36 (2016) 284-294.

[44] N.G. Khaligh, Res. Chem. Intermed. 41 (2015) 5411-5421.

[45] N.G. Khaligh, Chin. J. Catal. 35 (2014) 1497-1503.

[46] N.G. Khaligh, T. Mihankhah, M.R. Johan, J.J. Ching, J. Mol. Liq. 259 (2018) 260-273.

[47] E. Bartoszak-Adamska, Z. Dega-Szafran, A. Komasa, M. Szafran, Vib. Spectrosc. 81 (2015) 13-21.

[48] G.H. Silver, J.L. Wood, Trans. Faraday Soc. 60 (1964) 5-9.

[49] R. Ramasamy, J. Appl. Spec. 80 (2013) 492-498.

[50] N.P.G. Roeges, A Guide to the complete interpretation of infrared spectra of organic structures. Wiley, New York, 1994.

[51] R. A. Heacock, Léo Marion, Can. J. Chem. 34 (1956) 1782-1795.

[52] V. Krishnakumar, R. Ramasamy, Indian J. Pure & Appl. Phys. 40 (2002) 252-255.

[53] R. Ramasamy, Arm. J. Phys. 8 (2015) 51-55.

[54] Z. Dega-Szafran, M. Petryna, E. Tykarska, M. Szafran, Molecular structure of 1-piperidinium acid perchlorate studied by X-ray diffraction and FTIR spectroscopy. J. Mol. Structure 643 (2002) 69-75.

[55] T. Belhocine, S.A. Forsyth, H.Q.N. Gunaratne, M. Nieuwenhuyzen, P. Nockemann, A.V. Puga, K.R. Seddon, G. Srinivasan, K. Whiston, 3-Methylpiperidinium ionic liquids. Phys. Chem. Chem. Phys., 2015, 17, 10398-10416

[56] E.W. Garbisch, M.G. Griffith, J. Am. Chem. Soc. 90 (1968) 6543-6544.

[57] E. L. Eliel, S. H. Wilen and M. P. Doyle, Basic Organic Stereochemistry, Wiley-Interscience, New York, 2001, pp. 436-491.

[58] V.M.B. Nunes, M.J.V. Lourenco, F.J.V. Santos, C.N. de Castro, J. Chem. Eng. Data 48 (2003) 446-450.

[59] E. Hendriks, G.M. Kontogeorgis, R. Dohrn, J.C. de Hemptine, I.G. Economou, L.F. Zilnik, V. Vesovic, Ind. Eng. Chem. Res. 49 (2010) 11131-11141.

[60] F. Schneider, A. Stolle, B. Ondruschka, H. Hopf, Org. Process Res. Devel. 13 (2009) 44-48.

[61] N.G. Khaligh, S.B. Abd Hamid, S.J.J. Titinchi, Polycycl. Arom. Comp. 37 (2017) 31-38.

[62] E. Abbaspour-Gilandeh, S.C. Azimi, K. Rad-Moghadam, A.M. Barkchai, Iran. J. Catal. 3 (2013) 91-97.

[63] R.-Y. Guo, Z.-M. An, L.-P. Mo, R.-Z. Wang, H.-X. Liu, S.-X. Wang, Z.-H. Zhang, ACS Comb. Sci. 15 (2013) 557-563.

[64] S.S. Pendalwar, A.V. Chakrawar, A.S. Chavan, S.R. Bhusare, Der Pharma Chemica, 8 (2016) 143-145.

[65] G. Brahmachari, B. Banerjee, ACS Sustainable Chem. Eng. 2 (2014) 411-422.

[66] A. Shaabani, S. Samadi, Z. Badri, A. Rahmati, Catal. Let. 104 (2005) 39-43.

[67] M. Esmaeilpour, J. Javidi, F. Dehghani, F.N. Dodeji, RSC Adv. 5 (2015) 26625-26633.

[68] M. Khoobi, L. Ma'mani, F. Rezazadeh, Z. Zareie, A. Foroumadi, A. Ramazani, A. Shafiee, J. Mol. Catal. A: Chem. 359 (2012) 74-80.

[69] R. Teimuri-Mofrad, S. Esmati, S. Tahmasebi, M. Gholamhosseini-Nazari, J. Organometal. Chem. 870 (2018) 38-50.

[70] N. Hazeri, M.T. Maghsoodlou, F. Mir, M. Kangani, H. Saravani, E. Molashahi, Chin. J. Catal. 35 (2014) 391-395.

[71] A.C. Flores, E.A. Flores, E. Hernández, L.V. Castro, A. García, F. Alvarez, F.S. Vázquez, J. Mol. Liquids. 2014, 196, 249-257.

[72] X. Chen, W. Zhang, F. Yang, C. Guo, Z. Zhao, D. Ji, F. Zhou, Z. Wang, R. Zhao, L. Wang, Green Chem. Lett. Rev. 10 (2017) 54-58.

[73] A. Shaabani, S. Samadi, A. Rahmati. Syn. Commun. 37 (2007) 491-499.

[74] A.T. Khan, M. Lal, S. Ali, M.M. Khan, Tetrahedron Lett. 52 (2011) 5327-5332.

[75] J.M. Khurana, S. Kumar, Tetrahedron Lett. 50 (2009) 4125-4127.

[76] S. Abdolmohammadi, S. Balalaie, Tetrahedron Lett. 48 (2007) 3299-3303.

[77] M.G. Dekamin, M. Eslami, A. Maleki, Tetrahedron 69 (2013) 1074-1085.

[78] P. Das, A. Dutta, A. Bhaumik, C. Mukhopadhyay, Green Chem. 16 (2014) 1426-1435.

[79] M.M. Heravi, B.A. Jani, F. Derikvand, F.F. Bamoharram, H.A. Oskooie, Catal. Commun. 10 (2008) 272-275.

[80] M. Bihani, P.P. Bora, G. Bez, H. Askari, C. R. Chimie 16 (2013) 419-426.

[81] J. Zheng, Y. Li, Mendeleev Commun. 21 (2011) 280-281.

[82] S. Khaksar, A. Rouhollahpour, S.M. Talesh, J. Fluorine Chem. 141 (2012) 11-15.

[83] V. Bhaskar, R. Chowdary, S.R. Dixit, S.D. Joshi, Bioorg. Chem. 84 (2019) 202-210.

[84] S. Nemouchi, R. Boulcina, B.Carboni, A. Debache, C. R. Chimie 15 (2012) 394-397.

[85] S.S. Pourpanah, S.M. Habibi-Khorassani, M. Shahraki, Chin. J. Catal. 36 (2015) 757-763.

[86] D.S. Bhagat, J.L. Wawre, A.R. Yadav, P.G. Pathare, L. Kotai, R.P. Pawar, Eur. Chem. Bull. 6 (2017) 211-214.

[87] F. Shirini, M.S.N. Langarudi, N. Daneshvar, J. Mol. Liq. 234 (2017) 268-278.

[88] F. Shirini, N. Daneshvar, RSC Adv. 6 (2016) 110190-110205.

[89] K. Matuszek, A. Chrobok, F. Coleman, K.R. Seddon, M. Swadźba-Kwaśny, Green Chem 16 (2014) 3463-3471.

Highlights

- Synthesize of a low-viscous binuclear sulfonic-functionalized ionic liquid (SAIL)
- Measure and determine the physical properties
- Investigate the catalyst activity of new SAIL in the one-pot multicomponent reactions
- The present a new protocol for the synthesis using the planetary ball milling process
- The synthesis and characterization of new pyrano[4,3-*b*]pyrans